Received: 11 August 2020 | Revised: 6 October 2020 | Accepted: 6 October 2020

DOI: 10.1002/pen.25563

RESEARCH ARTICLE

POLYMER ENGINEERING AND SCIENCE WILEY

Evaluation of the salt leaching method for the production of ethylene propylene diene monomer rubber foams

Edoardo Zonta | Francesco Valentini | Andrea Dorigato | Luca Fambri | Alessandro Pegoretti

Department of Industrial Engineering and INSTM Research Unit, University of Trento, Trento, Italy

Correspondence
Francesco Valentini and Alessandro Pegoretti, Department of Industrial Engineering and INSTM Research Unit, University of Trento, Via Sommarive 9, Trento 38123, Italy.
Email: francesco.valentini@unitn.it (F. V.) and
Email: alessandro.pegoretti@unitn.it (A. P.)

Abstract

The thermomechanical behavior of ethylene propylene diene monomer (EPDM) foams produced with the salt leaching method has been investigated and compared with the behavior of EPDM foams obtained from conventional blowing agents. Moreover, the salt-leaching process has been optimized to minimize salt residues and the influence of different parameters (such as average particle size and particle size distribution) has been investigated. Scanning electron microscopy and density measurements highlighted that salt-leaching leads to the formation of open-cell porosity with cell dimensions of around 60 to 80 μm, while foams obtained with the two traditional foaming agents lead to closed-cell porosity. Compression set values indicate that the behavior of the foams produced with salt leaching are more similar to the unfoamed rubber, characterized by higher elasticity and low residual deformation. Two theoretical models were successfully applied to the compression curves (Mooney-Rivlin and Exponential-Logarithmic) and they highlighted the effect of foaming on the properties of EPDM rubber and in particular the higher chain extensibility obtained through the salt leaching foaming method.

KEYWORDS

blowing agents, density, foams, mechanical properties, model, processing, rubber

1 | INTRODUCTION

In the last few years, polymer foams have gained great interest due to their unique features. Due to the combination of low density and low thermal conductivity, these materials are mainly used for thermal insulation of residential, industrial, and commercial buildings.[1] The cellular structure of polymer foams influences their properties and allows considerable weight reduction, leading to economic advantages for various applications.[2] Moreover, modification in the cellular structure allow the optimization of the properties to satisfy the requirements for specific applications.[3-6] Polymer foams are expanded polymeric materials generally prepared using chemical or physical blowing agents.[7] In the case of physical blowing agents (such as water, hydrocarbons, chlorofluorocarbons, and hydrochlorofluorocarbons), the foaming agent is dissolved in the polymeric matrix and expands as a consequence of a pressure decrease or a temperature increase.[7] Chemical blowing agents are most commonly used and generally consist of a solid chemical added to the polymer matrix using an internal mixer or roller mills, and decomposes at a certain temperature generating a gas, which expands the matrix thus generating a cellular structure. Inorganic blowing agents (such as sodium and potassium carbonates) decompose endothermically and release CO_2 and H_2O with heat. Organic blowing agents (such as azodicarbonamide and

p,*p*'-oxybis-(benzene sulfonyl hydrazide)) decompose mainly exothermically and release nitrogen.[3,8,9] The porous structure is obtained through the nucleation of gas clusters in the material, as consequence of a pressure decrease, followed by the growth of pores in the polymer until they reach an equilibrium size. The foam density depends on several factors, such as the original gas concentration, the gas fraction that remains dissolved in the polymer matrix and the depressurization rate.[10,11] Depending on the foaming parameters, foams can be characterized by open-cell and/or closed-cell porosity.[12]

Expanded rubbers are materials consisting of a rubber matrix and a porosity containing a gaseous phase (generally air). Depending on the morphology of the pores (ie, open-cell and/or closed-cell structure), these materials could find several applications, ranging from thermal insulators, gaskets and impact sound deadening products.[13-15] Rubber foams have been successfully made from natural rubber[16-18] as well as synthetic rubbers such as styrene-butadiene rubber,[19,20] acrylonitrile butadiene rubber (NBR),[21,22] chlorinated polyethylene rubber,[23] polychloroprene rubber,[24] and ethylene propylene diene monomer (EPDM) rubber.[21,25,26] EPDM is a synthetic rubber made from ethylene and propylene polymerized with a nonconjugated diene monomer and it is one of the most widely used elastomers.[27] EPDM rubber compounds are generally obtained by mixing the EPDM rubber with vulcanizing agents, antioxidants, activators, fillers (mainly carbon black), and accelerators.[28] After vulcanization, the resulting materials are characterized by good mechanical properties, high resistance to aging, ozone, UV, and weathering. On the other hand, they are also characterized by a poor resistance to polar fluids and oils. EPDM foams are used in the production of gaskets, O-rings, window seals, belts, electrical insulation of cables, and waterproofing membranes.[29,30]

Despite the extensive use of chemical foaming agents for the production of expanded polymers, many of them are hazardous for health and their use is not allowed in the EU.[9] For this reason, safer foaming agents, such as physical foaming agents like water or hydrocarbons are often required.[31,32] The main limitation related to physical foaming agents consists in the need of additional machinery and thus in a more complex process, with a consequent cost increase.[9] Because of these problems, a possible alternative to traditional foaming agents is "particle leaching" which involves the addition of water-soluble solid particles (such as sodium chloride and potassium chloride) into the polymer matrix and their subsequent dissolution in hot water, leading to the formation of a porous cellular network throughout the polymer matrix.[33-36] This technology has been commonly used for the production of ecofriendly scaffolds, because the resulting pore size is optimal for scaffolds,[34,35,37] and for the production of plastic semiconductors.[38] Particle leaching has been used for the production of monolayer NBR rubber stamps[39] and for tissue engineering applications and for the production of soft sensors, both with silicon rubber.[40]

Despite the environmental advantages deriving from the production of elastomeric foams using particle leaching, only a few studies can be found in the open literature on this topic.[39,40] Moreover, no papers dealing with the production and the investigation of the mechanical and thermal properties of EPDM foams produced with this technology have been published. This work is focused on the production of EPDM foams using the technique of particle leaching; the optimization of the production process and the investigation of the thermal and mechanical properties of the resulting foams. EPDM foams produced with two different kinds of traditional blowing agents have been compared to the particle leached foams.

2 | EXPERIMENTAL PART

2.1 | Materials

A Vistalon 2504 EPDM rubber, containing 58 wt% of ethylene and 4.7 wt% of ethylidene norbornene, with a Mooney viscosity (ML 1 + 4, 125°C) of 25 MU, was purchased from Exxon Mobil (Irving, TX). Zinc oxide (curing activator), stearic acid (curing activator and lubricating agent) and sulfur (vulcanizing agent) were supplied by the Rhein Chemie (Cologne, Germany). The accelerators, tetramethylthiuram disulfide (TMTD), and zinc dibutyl dithiocarbamate (ZDBC) were obtained from the Vibiplast srl (Castano Primo [MI], Italy). Carbon black N550, purchased from the Omsk Carbon group (Omsk, Russia), was used as reinforcing filler. Polyethylenglycol (PEG), having a molecular weight of 2000 Da, was acquired from the Alfa Aesar (Kandel, Germany). The composition of the elastomeric compound used for the preparation of the samples (the quantities are expressed in "per hundred rubber" [phr]) is given in Table 1.

Sodium chloride (density 2.16 g/cm^3), commercial grade, was grinded and sieved into eight fractions: granulometry <60 μm, <150 μm, 60 to 80, 80 to 100, 100 to 150, 150 to 300, 300 to 800 and >800 μm (corresponding to 230, 100, 230, 200, 140, 100, 50, 20 mesh sieves, respectively). The salt particles were then dried and stored in an oven at 60°C until use. The method described by Scaffaro et al.[35] was adapted for the determination of

TABLE 1 Composition of the EPDM elastomeric compound used for the preparation of the samples

Material	Quantity (phr)
Vistalon® 2504	100
Sulfur (vulcanizing agent)	3
Zinc oxide (activator)	3
Stearic acid (activator)	1
Carbon black (reinforcing filler)	20
TMTD (accelerator)	0.87
ZDBC (accelerator)	2.5

Abbreviations: TMTD, tetramethylthiuram disulfide; ZDBC, zinc dibutyl dithiocarbamate.

the quantity of PEG, the quantity of salt, and the procedure for salt dissolution.

Two different traditional foaming agents were considered in this work: Micropearl F82 obtained from the Lehvoss Italia S.r.l. (Saronno, Italia) and Expancel 909DU80 purchased from the Nouryon Chemicals spa (Milano, Italy). The two foaming agents consisted of microspheres containing a low-boiling-point hydrocarbon that, increasing the temperature above 120 to 130°C, start expanding due to the vaporization of the hydrocarbon. In preliminary studies the density of the foams as a function of the blowing agent concentration was investigated and an optimal concentration of 14 phr (9.7 wt%) was assessed in order to obtain the lowest density values.[41]

2.2 | Sample preparation

EPDM foams were prepared by melt compounding in an internal mixer (Thermo Haake Rheomix 600), equipped with counter rotating rotors. The compounding process was optimized as follows: the temperature was fixed at 40°C in order to maintain adequate rubber viscosity, while the rotor speed was set at 50 rpm for improving salt dispersion. First, EPDM was fed into the mixer with the carbon black and mixed for 5 min, then the vulcanizing agent and the additives were added and mixed for other 5 min in order to obtain a homogeneous compound. Then the procedure was different for the four samples, as follows:

- To produce the unfoamed EPDM reference sample, after a mixing time of 10 min, the material was vulcanized in a closed mold at a pressure of 8 bar and a temperature of 170°C for 20 min. In this way, square sheets ($110 \times 110 \times 5$ mm^3) were obtained.
- To produce the Expancel and the Micropearl foam samples, the foaming agent was then added and mixed for 5 min, thus obtaining a total mixing duration of 15 min. According to our previous work[41] the vulcanization process of the resulting compounds was carried out in a closed mold at a pressure of 2 bar and a temperature of 170°C. After 10 min the pressure was released in order to allow the expansion of the material, and the samples were left for further 10 min in order to allow the completion of the vulcanization process. In this way, square sheets ($110 \times 110 \times 10$ mm^3) of the foamed blends at different relative compositions were obtained.
- The production process used for the preparation of samples using salt leaching is schematically represented in Figure 1. Initially, NaCl and PEG were gradually added into the mixer in order to obtain a fine, homogeneously dispersed powder, reaching a total mixing duration of 15 min. The vulcanization process of the resulting compounds was carried out in a closed mold under a pressure of 2 bar and at a temperature of 170°C for 20 min. Finally, NaCl and PEG were removed by leaching in a bath of demineralized water at a temperature of 80°C for 3 h, leading to the formation of a porous cellular network in the elastomeric matrix. The samples where then dried overnight in an oven at 60°C. In this way, square sheets ($110 \times 110 \times 5$ mm^3) were obtained.

The list of the prepared foams with their codes is given in Table 2. The sample named "EPDM" refers to the unfoamed EPDM rubber. It should be noticed that for each sample a different quantity of material was used in order to fill the mold, for this reason the amount of polymer (Vistalon 2504) used in each composition is reported. The name of samples obtained by salt leaching is composed by the term NaCl followed by the size of the salt used for the production. The sample NaCl 50/50 was produced using 50 wt% of salt particles with size 60 to 80 μm and 50 wt% of salt with size 80 to 100 μm.

2.3 | Experimental methodologies

2.3.1 | Residual salt and connectivity measurements

The amount of residual salt after leaching has been calculated according to Equation (1):

$$\text{Residual salt}\,(\%) = \frac{m_{\text{dry}} - m_{\text{tot}}}{m_{\text{dry}}} \times 100 \qquad (1)$$

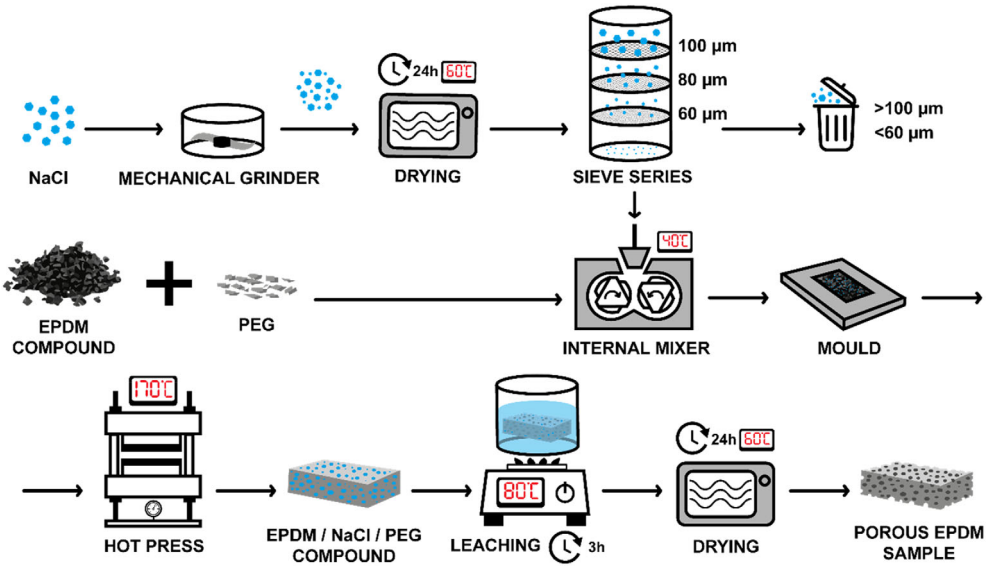

FIGURE 1 Production process of ethylene propylene diene monomer (EPDM) foams by the salt leaching method. PEG, polyethylenglycol [Color figure can be viewed at wileyonlinelibrary.com]

TABLE 2 List of the prepared samples

Sample	Vistalon® 2504 (g)	Expancel 909DU80 (phr)	Micropearl F82 (phr)	NaCl (phr)	PEG (phr)	Salt granulometry (µm)
EPDM	50	—	—	—	—	—
Expancel	15	14	—	—	—	—
Micropearl	15	—	14	—	—	—
NaCl 60-80	13.6	—	—	305	30	60–80
NaCl 80–100	13.6	—	—	305	30	80–100
NaCl 50/50	13.6	—	—	305	30	50 wt% 60–80 50 wt% 80-100

Abbreviations: EPDM, ethylene propylene diene monomer; PEG, polyethylenglycol.

where m_{dry} is the mass of the material after the drying process subsequent to the leaching and m_{tot} is the theoretical mass of the material in the case of complete salt dissolution evaluated according to Equation (2):

$$m_{tot} = m_0 - m_{NaCl} - m_{PEG} \quad (2)$$

where m_0 is the mass of the material before the dissolution in water (equal to 63.29 g), m_{NaCl} and m_{PEG} are the mass of NaCl (41.48 g) and of PEG (4.08 g), respectively.

With the aim of evaluating the continuity of the porosity and therefore the dissolution of the foaming agents (PEG, NaCl), also the connectivity (C) has been calculated according to Equation (3):[35]

$$C = \frac{(m_0 - m_{dry})}{m_{NaCl} + m_{PEG}} \times 100 \quad (3)$$

2.3.2 | Water uptake measurements

Water uptake measurements were carried out in order to identify the influence of the porosity dimension on the ability of the materials to absorb water. The test was conducted using demineralized water and the mass was measured using a Kern KB3600 balance (resolution of 10 mg). For each sample the measure was carried out two times: after 2 h and after 24 h of immersion in water. The test was carried out following the procedure reported in the ASTM D570-98: drying for 24 h in oven at 50°C, weighing, immersion in water for 2 h, weighing, immersion in water for further 22 h, weighing. The percentage of material filled by water (the water uptake [W.U.]) has been calculated according to Equation (4):

$$W.U. = \frac{m_{wet,x} - m_{dry}}{m_{dry}} \times 100 \quad (4)$$

where $m_{wet,x}$ is the mass of the sample after the immersion in water (x represents the time of immersion: 2 and 24 h) and m_{dry} is the mass of the sample after the drying process subsequent to the leaching process (ie, the mass of the sample before the test).

2.3.3 | Scanning electron microscopy

Cryofractured surfaces of the foams were observed through a Zeiss Supra 40 field emission scanning electron microscope (FESEM), operating at an accelerating voltage of 3 kV. Prior to measurement, the samples were metallized through the deposition of a thin electrically conductive coating of platinum palladium inside a vacuum chamber.

2.3.4 | Density measurements

Helium pycnometry density (ρ_{picn}) measurements were conducted using a gas displacement AccuPycII 1330 pycnometer (Micrometrics Instrument Corporation) at a temperature of 23°C. For each sample 30 replicate measures were performed. A measure of the geometrical density (ρ_{geom}) (ie, mass over the total volume inclusive of solid, closed, and open porosity [OP]) was carried out on five cylindrical specimens by measuring the mass with a Gibertini E42 balance (0.1 mg sensitivity) and the dimensions using a caliper (resolution of 0.01 mm). According to ASTM D6226 standard, it was possible to calculate the total porosity (P_{tot}) and the fraction of OP and close porosity (CP) according to Equations (5), (6), and (7):

$$P_{tot} = \left(1 - \frac{\rho_{geom}}{\rho_{bulk}}\right) * 100 \quad (5)$$

$$OP = \left(1 - \frac{\rho_{geom}}{\rho_{picn}}\right) * 100 \quad (6)$$

$$CP = P_{tot} - OP \quad (7)$$

where ρ_{bulk} is the density of the material without porosity (ie, 1.042 g/cm^3 for the unfoamed EPDM sample, in agreement to values reported in the literature[1]).

2.3.5 | Thermogravimetric analysis

Investigation of the thermal degradation behavior of the prepared materials was carried out through thermogravimetric analysis (TGA) in order to assess the influence of the foaming process on the degradation resistance of the materials and to evaluate any residual foaming agent at high temperature (for Micropearl and Expancel samples) and of porogen agents (for the NaCl 60-80 sample). TGA was performed through a TGA TA-I Q5000 IR thermobalance under a nitrogen flow of 10 ml/min in a temperature interval between 30 and 700°C, at a heating rate of 10°C/min. The temperature associated to a mass loss of 2% ($T_{2\%}$), the temperatures associated to the maximum rate of degradation (T_{peak1}, T_{peak2}), the residual mass at 250°C (m_{250}), the residual mass at 415°C (m_{415}), the residual mass at 500°C (m_{500}), and the residual mass at 700°C (m_{700}) were determined.

2.3.6 | Thermal conductivity measurements

Thermal conductivity tests were carried out by using the guarded hot plate configuration, according to ASTM E1225-13 standard.[42] A laboratory set-up equipped with a heated plate, a cooled plate and two references plates (see the set-up scheme reported in Figure 2) was utilized. The two aluminium plates were maintained at a temperature of 45.0 ± 0.5°C and 5.0 ± 0.5°C, respectively, by using two laboratory water baths. Two polymethylmethacrylate (PMMA) plates, with a thermal conductivity of 0.235 W/m K and dimensions of 110 × 110 × 10 mm^3 were used as reference. The temperature at each interface was monitored using six thermocouples (sensitivity of 0.25°C, diameter of the wires equal to 0.075 mm), fixed on the specimen surface using conductive adhesive tapes. Temperature data were acquired using an Arduino Mega (Arduino srl, Genova-Italy) equipped with a Module MAX6675 interface. The testing chamber was insulated from the external environment using an insulation box made of expanded polystyrene.

The thermal conductivity was calculated according Equation (8):

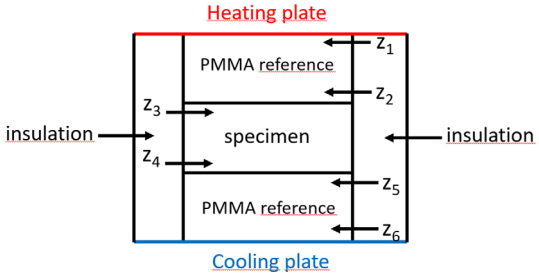

FIGURE 2 Scheme of the set-up used for the evaluation of the thermal conductivity (adapted from ASTM E1225-13 [42]) [Color figure can be viewed at wileyonlinelibrary.com]

$$k_S = \frac{Z_4 - Z_3}{T_4 - T_3} \cdot \frac{k_M}{2} \cdot \left(\frac{T_2 - T_1}{Z_2 - Z_1} + \frac{T_6 - T_5}{Z_6 - Z_5} \right) \quad (8)$$

where k_s is the thermal conductivity of the material, k_M is the thermal conductivity of a reference material, Z_i is the distance of the thermocouple "i" from the top of the highest reference, T_i is the temperature of the thermocouple "i".In order to reach a steady-state condition the test duration was of 3 h and only the temperature values referring to the last 15 min were used for the calculation of the thermal conductivity. The measurements were carried out on specimens with dimensions of $110 \times 110 \times 10$ mm^3.

As a comparison, thermal conductivity tests were also carried out according to ISO22007-02 on squared specimens with dimensions equal to $50 \times 50 \times 10$ mm^3 by using a Hot Disk thermal analyser equipped with a 5501 sensor. The test was performed at a temperature of 23 ± 1°C, applying for 40 s a power of 30 mW in the case of unfoamed EPDM and of 15 mW for the other samples. These operating parameters were chosen in order to guarantee a thermal increase of each specimen of at least 2°C, as reported in the standard (for this reason, in the case of EPDM, due to the higher thermal conductivity, a higher power was necessary). At least three measurements were performed for each sample.

2.3.7 | Quasi-static compression test and shore hardness measurements

Compressive properties under quasi-static conditions were measured on square specimens with dimensions equal to $50 \times 50 \times 10$ mm^3 using an Instron 5969 tensile testing machine equipped with a load cell of 10 kN and operating at a cross-head speed of 1 mm/min. The compressive modulus, normalized by the geometrical density of each samples, was measured as a secant value between strain levels of 0.1 and 0.2 mm/mm for the foamed samples, while for unfoamed EPDM sample it was determined as a secant value between stress levels of 20 and 25 MPa. The deformation of the different samples corresponding to a stress equal to 5 MPa (ε_5) has been also evaluated. Moreover, for the foamed samples, the stress values (normalized by the density of each sample) corresponding to a deformation equal to 0.15 mm/mm ($\sigma_{0.15}$) and to 0.35 mm/mm ($\sigma_{0.35}$) have been calculated. At least five specimens were tested for each composition. Shore A hardness test was performed using a Hilderbrand Durometer following the ASTM D2240 standard. Square samples 20 mm wide and 10-mm thick (5 mm in case of unfoamed EPDM sample) were tested, and at least 10 measurements were performed for each composition. The Shore A value was determined after pressing the indenter against the specimen for a time equal to 10 s.

2.3.8 | Compression set measurements

Compression set measurements were carried out according to ASTM D395-85 standard for 22 h at a temperature of 23°C. Recovery measurements were made after 30 min. The test samples had a diameter of 12 mm for unfoamed EPDM and NaCl 60-80, and of 28 mm for Micropearl and Expancel foams. The ratio between the thickness of the samples and the thickness of the spacing bars was equal to 1.3333. The compression set (Cb) has been evaluated according to Equation (9):

$$\mathrm{Cb} = \frac{t_0 - t_i}{t_0 - t_u} \times 100 \quad (9)$$

where t_0 is the initial thickness of the specimen, t_i the final thickness, and t_u the thickness of the spacing bars.

3 | RESULTS AND DISCUSSION

3.1 | Preliminary considerations regarding the salt leaching method

To reach a suitable method for the production of foamed samples through salt leaching, the effect of various processing parameters has been investigated and a repeatable and reliable preparation method has been defined. The main parameters affecting the properties of the foams are (a) the salt granulometry, (b) the humidity content of the salt, (c) the quantity of material filling the mold, and (d) the mold thickness.

Salts with granulometry higher than 100 μm produced inhomogenous samples with large salt grains separated from the rubber matrix. Samples with salt sizes in the range 300 to 800 μm, 150 to 300 μm, and 100 to 150 μm were friable and easily crumbled even during the dissolution of the porogenic agent in water. Mechanical properties of these samples were thus very poor and not uniform across the specimens. Figure 3(A,B) show some samples prepared with salt granulometry greater than 100 μm.

Samples produced using salt with granulometry lower than 60 μm have been discarded because the compounded material, before vulcanization, was inhomogeneous and showed distinct agglomeration of compact rubber surrounded by salt powder not included in the

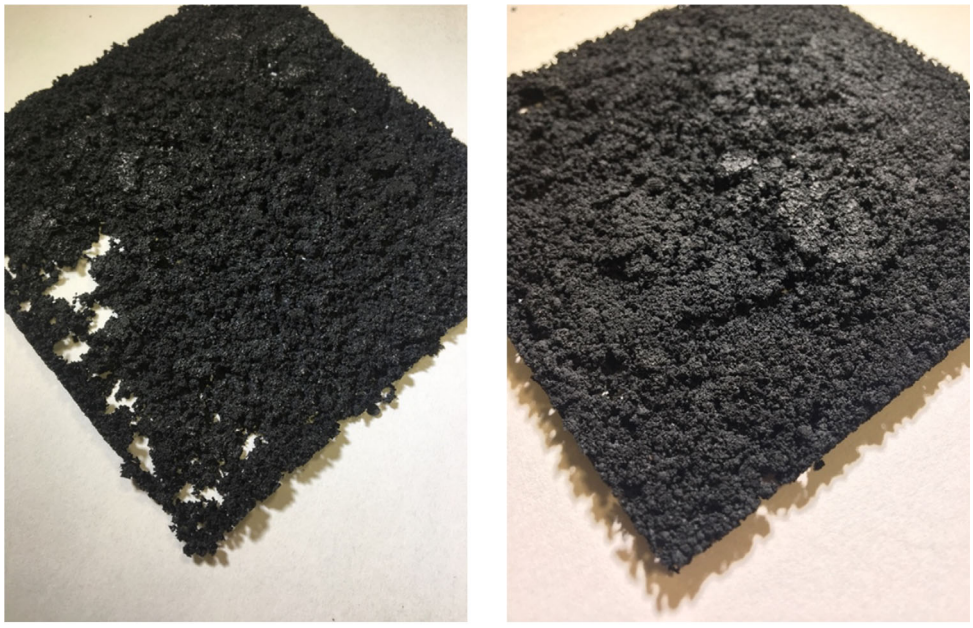

FIGURE 3 Samples produced with salt granulometry higher than 100 μm: 300 to 800 μm (A); 150 to 300 μm (B) [Color figure can be viewed at wileyonlinelibrary.com]

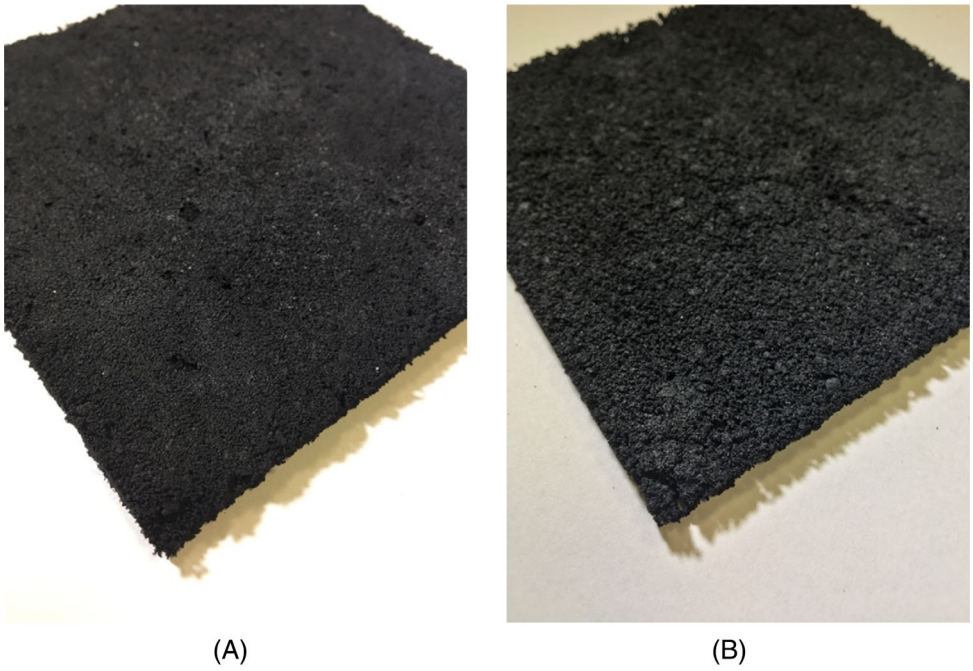

FIGURE 4 Samples produced with salt granulometry (A) between 100 and 150 μm, (B) lower than 150 μm [Color figure can be viewed at wileyonlinelibrary.com]

mesh. This structure remained after vulcanization and led to poor homogeneity of the morphology. One possible reason for this behavior was that the surface interaction established between salt and rubber was too strong; the adhesion seemed to increase as the granulometry decreased.

Moreover, the granulometric distribution of the salt must be precisely controlled: the presence of small quantities of salt outside the acceptable particle size region lead to strong inhomogeneities in the morphology of the samples. This behavior was observed comparing two samples produced by using respectively a salt grain size in the range 100 to 150 μm or simply lower than 150 μm (ie, obtained using only a 150 μm sieve). As shown in Figure 4(A,B), sample produced with a defined salt granulometry (100-150 μm) appeared visually more homogeneous that the one with all sizes less than 150 μm, with a better continuity of the rubber matrix.

Another factor that can lead to the production of inhomogeneous samples is the presence of water in the

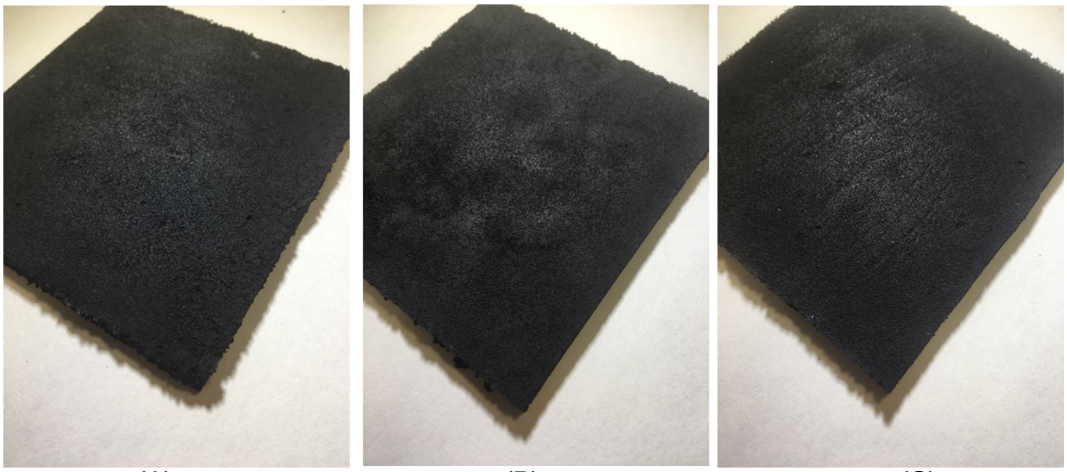

FIGURE 5 Samples produced by salt leaching: (A) NaCl 50/50, (B) NaCl 80-100, (C) NaCl 60-80 [Color figure can be viewed at wileyonlinelibrary.com]

TABLE 3 m_{tot}, m_{dry}, residual salt and connectivity values obtained for the samples produced through salt leaching

Sample	m_{tot} (g)	m_{dry} (g)	Residual salt (wt%)	Connectivity (%)
NaCl 80–100	17.73	19.65	9.8	95.8
NaCl 60–80	17.73	19.18	7.6	96.8
NaCl 50/50	17.73	19.31	8.2	96.5

salt, as the absorbed water increases with the specific surface area of the salt, that is, increases as the granulometry decreases. Humidity absorbed by salt negatively affected the homogeneity of the compound and caused an undesired expansion during the vulcanization, due to the evaporation of the water trapped inside the elastomeric matrix. Hence, the sieved salt was stored in a ventilated oven at 60°C at least for 24 h before use. On the other hand the absorption of water in the EPDM matrix can be excluded because this rubber has very low water absorption values [43].

The quantity of material filling the mold was another important parameter controlled in the preliminary evaluation stage of the samples. The mold must be filled homogenously with an optimal quantity of material to avoid the formation of dense regions in case of excess of material, or the formation of voids and discontinuities in the elastomeric matrix in case of scarcity of material. If an excessive quantity of filling material was used, PEG escaped from the polymeric matrix during compression molding and the dissolution of the porogenic agents was inhibited and significant residual salt remained in the samples.

Finally, the thickness of the mold should not be lower than 5 mm to prevent densification, porosity inhomogeneity, and residual salt; therefore a mold thickness of 5 mm (raised to 10 mm in order to produce specimens suitable for the compression tests) was used.

As a result of the above mentioned issues, only some samples were selected for the characterization: NaCl 80-100, NaCl 60-80, NaCl 50/50 (as given in Table 2). In Figure 5(A-C) representative images of these three samples are shown.

3.2 | Characterization of the samples

3.2.1 | Residual salt and connectivity measurements

Table 3 shows the residual salt and the connectivity values obtained for samples NaCl 80-100, NaCl 60-80, and NaCl 50/50 produced through salt leaching.

3.2.2 | Water uptake measurements

Residual salt is a minimum for the NaCl 60-80 sample (7.6 wt%), a maximum for the NaCl 80-100 (9.8 wt%) while the sample produced with a mix of the two grain sizes (ie, NaCl 50/50) shows an intermediate value. These data are consistent with the values of connectivity given in Table 3. These results confirm that the salt granulometry determines the porosity of the resulting foam and affects the effectiveness of the dissolution phase. These data are well correlated to results obtained from

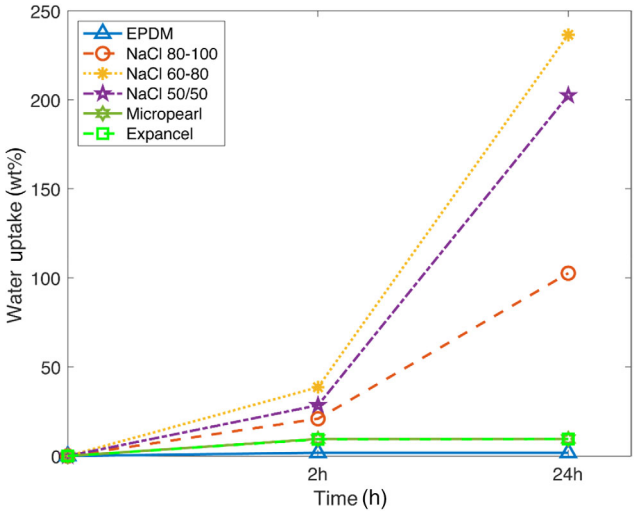

FIGURE 6 Results of the water uptake test after 2 and 24 h. EPDM, ethylene propylene diene monomer [Color figure can be viewed at wileyonlinelibrary.com]

TABLE 4 Mass values used for the calculation of the water absorption values

Sample	m_{dry} (g)	$m_{wet,\ 2\ h}$ (g)	$m_{wet,\ 24\ h}$ (g)
EPDM	53.28	54.24	54.29
NaCl 80–100	19.65	23.76	39.81
NaCl 60–80	19.18	26.58	64.55
NaCl 50/50	19.31	24.81	58.41
Expancel	18.00	19.68	19.72
Micropearl	19.68	21.55	21.57

Abbreviation: EPDM, ethylene propylene diene monomer.

water uptake tests as shown in Figure 6 (mass values used for the calculation are given in Table 4); that is, as the salt granulometry decreases, the size of the porosity and consequently the quantity of water absorbed increases.

Expancel and Micropearl foams are characterized by low absorption values (of around 9%) due to the closed porosity originated by the use of microcapsules (see Figure 8(D-E)) and the water absorption values do not change over time. Different absorption values between samples obtained through salt leaching and samples obtained using commercial foaming agents could be due to the presence of residual salt that increases the polarity of the material resulting in a higher amount of absorbed water. The contribution of the EPDM matrix to the water uptake can be neglected, because of its limited water absorption capability (of around 2%), that is confirmed by the literature data.[43]

3.2.3 | Scanning electron microscopy

Scanning electron microscopy (SEM) observations were performed to analyse morphological features of the produced samples and to assess the effectiveness of the dissolution phase in samples produced through salt leaching. Micrographs show that the structure obtained through salt leaching (Figure 7(A-C) and Figure 8(A-C)) is very different from the morphology of Micropearl and Expancel (Figure 8(D-E)). For the former, the porosity is open, highly interconnected and with slightly smaller pore dimensions; cells boundaries cannot be distinguished and the morphology is similar to a continuous phase in the elastomeric matrix. Moreover a slight decrease in the dimension of the porosity is evident as the granulometry of salt employed decrease. No visible residues of salt in NaCl 80-100, NaCl 60-80, and NaCl 50/50 were present.

The obtained morphology is different respect to other elastomeric foams present in the literature using the same technique (such as the NBR foam obtained by Trakanpruk[39]), mainly due to the strong dependency of the porosity on the salt size that is used for the leaching process. In particular, the salt granulometry that has been used in this work created a porosity with higher dimensions (in their case the salt size was around 30 μm). The morphology is not very different respect to the morphology that can be obtained applying this technique to the foaming process of thermoplastics: Scaffaro[35] showed similar morphology in the case of using salt with granulometry in the range 90 to 110 μm.

On the other hand, the use of Expancel 909DU80 and Micropearl F82 as foaming agents leads to the formation of close cells, homogeneously distributed within the matrix, with a mean size within 60 and 80 μm. Microsphere residues are still visible inside some broken cells.

3.2.4 | Density measurements

To correlate the morphology of the different samples with their porosity values, density measurements were performed and are given in Table 5. Samples produced through salt leaching are characterized by ρ_{picn} values much higher that ρ_{geom} values due to the high content of OP in these materials. Calculations regarding samples produced with the salt leaching method were performed assuming that the total porosity was equal to the OP. Note that the values given are lower bounds since any unleached salt would lead to higher values of OP due to salt's higher density (2.16 g/cm^3)[44] with respect to the EPDM matrix. Expancel and Micropearl samples have

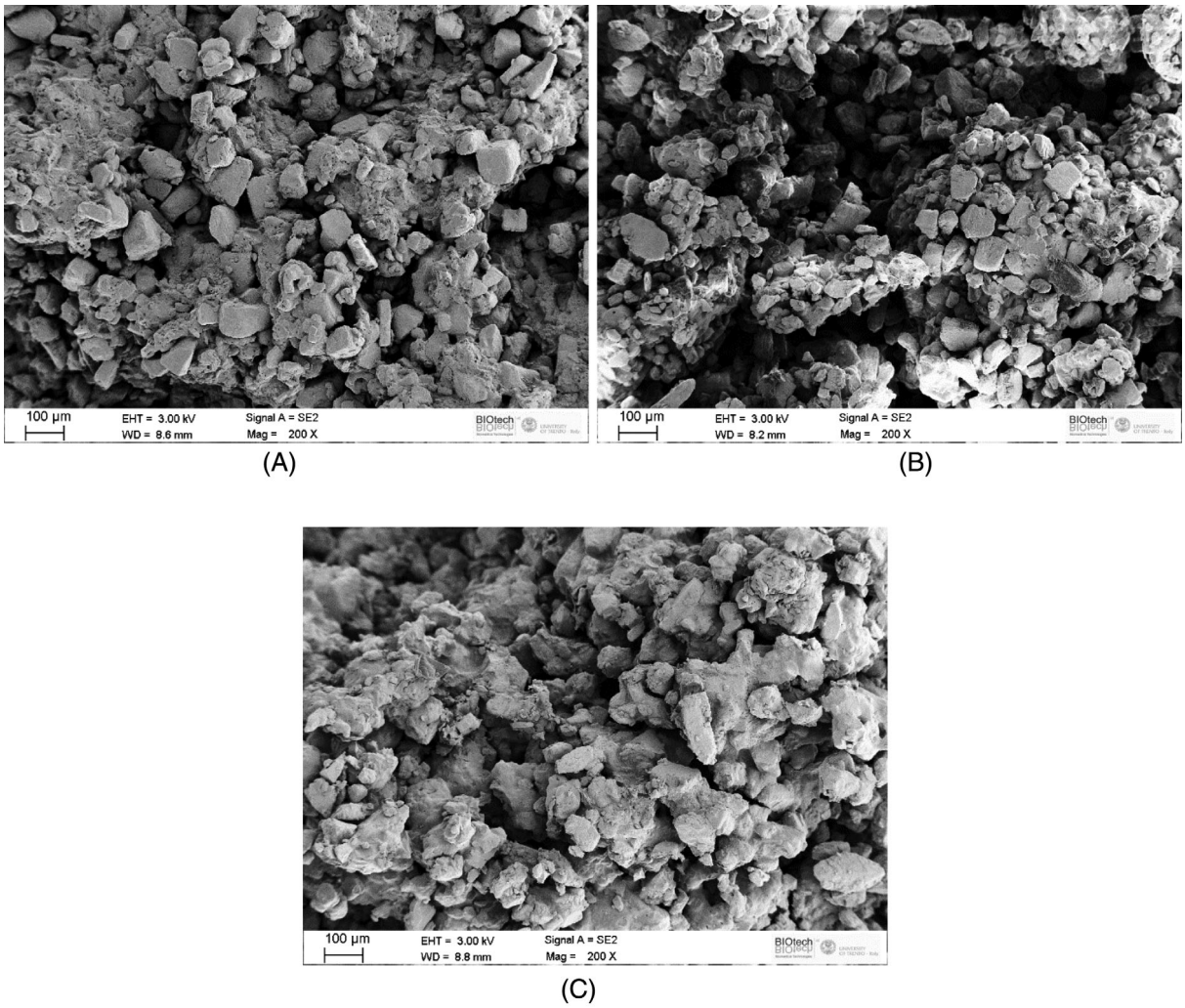

FIGURE 7 Scanning electron micrographs at 200× of the prepared foams: (A) NaCl 80-100, (B) NaCl 60-80, (C) NaCl 50/50

higher porosities, mainly with closed structure. ρ_{geom} values indicate that the use of Expancel 909DU80 and Micropearl F82 as foaming agents leads to lower density values with respect to the use of salt leaching. The density values are quite different; the lowest density value is obtained for the Micropearl sample (0.226 g/cm^3) while the lowest value from salt leaching is from the NaCl 50/50 foam (0.390 g/cm^3). The latter sample also presents the highest porosity (66.3%).

Although the P_{tot} values of NaCl 60-80 and NaCl 50/50 are very similar, the water uptake values (reported in Figure 6) are very different with the former able to absorb a higher amount of water. The smaller pores and higher connectivity are likely responsible for the absorption of a higher quantity of water. NaCl 60-80 was therefore selected for further testing, due to higher connectivity, higher water sorption, and lower salt residue.

3.2.5 | Thermogravimetric analysis

Thermogravimetric curves along with the corresponding derivative curves are presented in Figure 9(A,B) while the most significant results are given in Table 6.

TGA curves of Micropearl and Expancel expanded rubbers are similar to that of unexpanded rubber. An initial weight loss of about 2% to 3% is observed in the range 180 to 230°C corresponding to the evaporation of low molecular weight plasticizers and oils commonly used in rubber production. The main degradation of rubber starts at around 280°C, evidencing a maximum degradation rate at about 460°C, with a slight shift between pristine EPDM and the rubbers with Micropearl and Expancel. From 500 to 580°C, the mass loss of the final residues of rubbery components of Micropearl and Expancel and pristine EPDM are present. The thermolysis of CB starts at about 580°C for Micropearl, and at about 610°C for

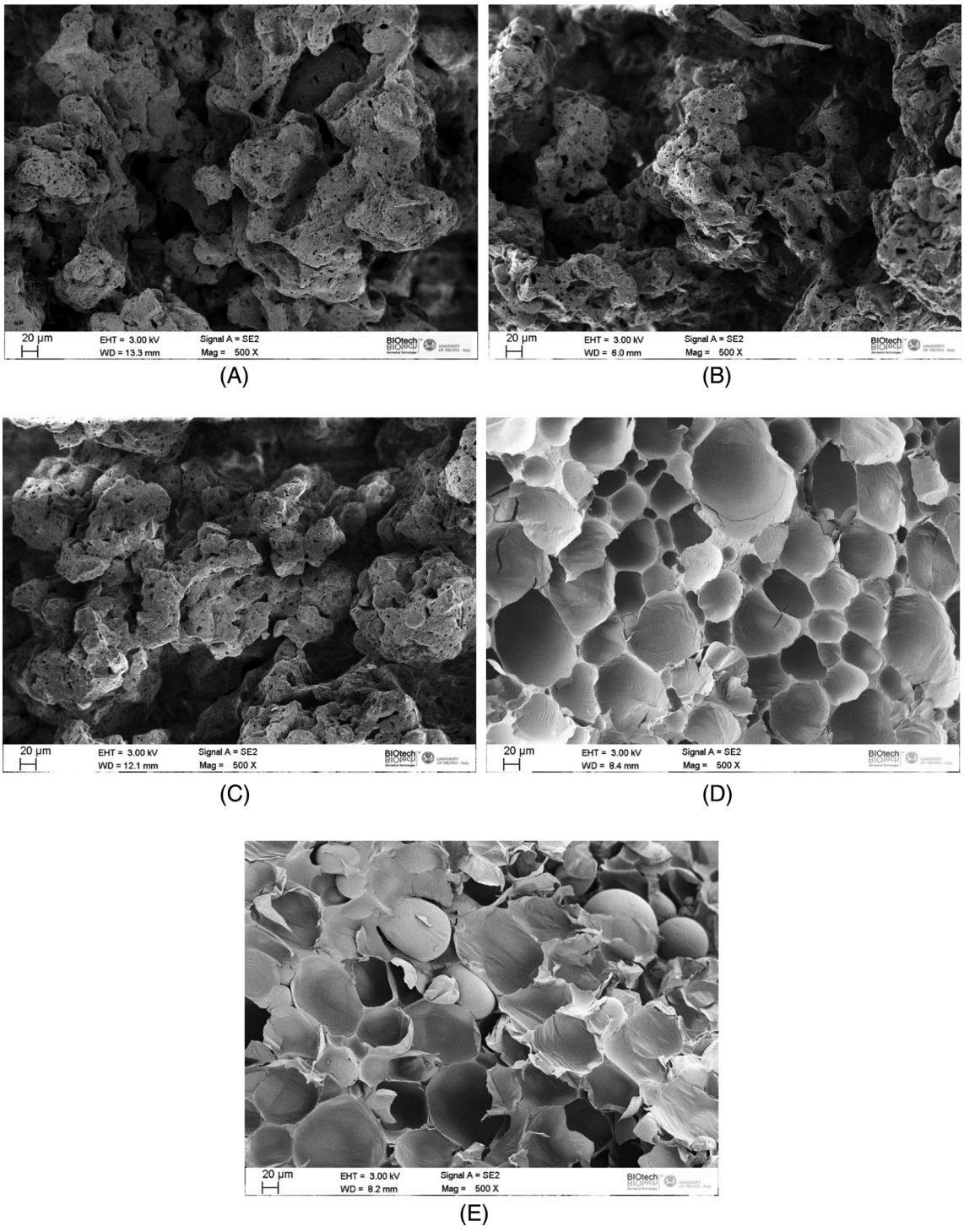

FIGURE 8 Scanning electron micrographs at 500× of the prepared foams: (A) NaCl 80-100, (B) NaCl 60-80, (C) NaCl 50/50, (D) Micropearl, (E) Expancel

pristine EPDM and Expancel. Considering the residue at 700°C (m_{700}), these samples show a minimum residual mass of about 3.5 wt%, corresponding to the typical concentration of inorganic by-products derived from degradation of common additives of rubber compounds. Foamed rubbers evidenced a significant decrease of their thermal stability in the temperature range 250 to 415°C from about 10% without foaming to about 20% in the case of Micropearl and Expancel, and 46% in the case of NaCl 60-80. This behavior can be justified by the increased surface area exposed to degradation, the presence of pathways for release of by-products, and by oxidative

TABLE 5 Density and porosity values of the prepared samples

Sample	ρ_{geom} (g/cm^3)	ρ_{picn} (g/cm^3)	P_{tot} (%)	OP (%)	CP (%)
EPDM	1.042 ± 0.005	1.001 ± 0.002	0	0	0
NaCl 80–100	0.420 ± 0.002	1.151 ± 0.016	63.5	63.5	—
NaCl 60–80	0.409 ± 0.018	1.166 ± 0.022	64.9	64.9	—
NaCl 50/50	0.390 ± 0.004	1.159 ± 0.015	66.3	66.3	—
Expancel	0.242 ± 0.012	0.378 ± 0.022	75.8	35.9	39.9
Micropearl	0.226 ± 0.024	0.360 ± 0.014	77.4	37.8	39.6

Abbreviations: CP, close porosity; EPDM, ethylene propylene diene monomer; OP, open porosity.

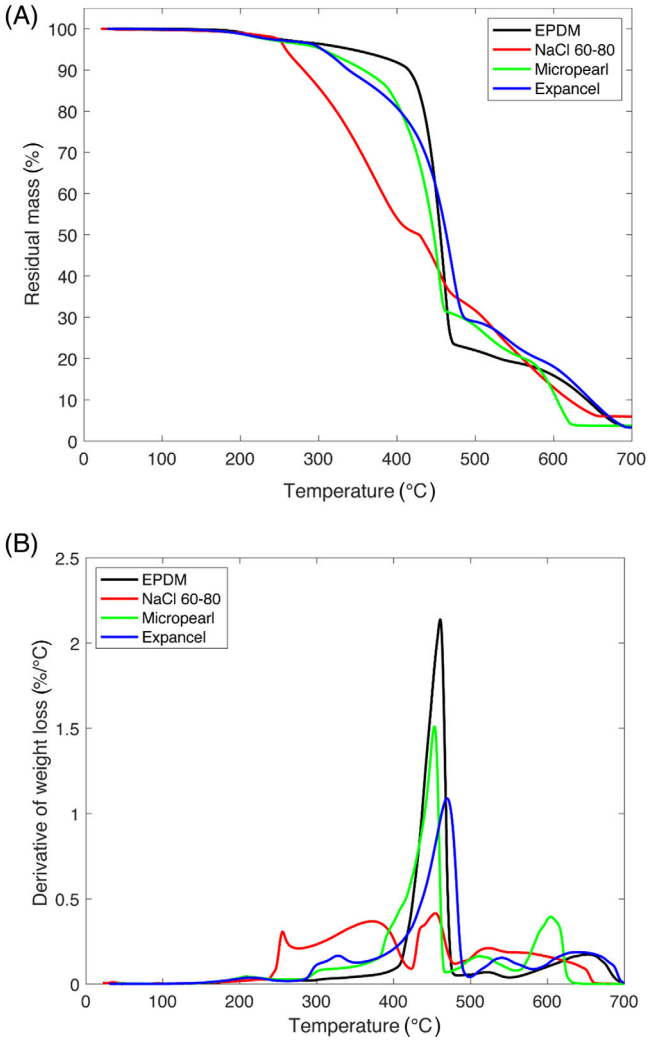

FIGURE 9 Residual mass (A) and derivative of mass loss (B) from thermogravimetric analysis tests. EPDM, ethylene propylene diene monomer [Color figure can be viewed at wileyonlinelibrary.com]

processes due to the presence of air trapped in the porosity.[45] These effects are amplified in the case of NaCl 60-80 due to the presence of OP that represents a weaker barrier against gas release and offers a higher surface exposed to the degradation. The TGA thermogram of uncured EPDM compound (not shown for the sake of brevity) is perfectly overlapping to that of vulcanized EPDM rubber up to 400°C.

The amount of degradation that occurs from 415 to 500°C is inverse with respect to degradation at lower temperature. Specifically, the amount of degradation is highest in the case of the unfoamed EPDM sample (67.7%) but is lower for foamed samples, that is, about 48% for Micropearl and Expancel, and 19.3% for NaCl 60-80. The peculiar behavior of the NaCl 60-80 with respect to unfoamed EPDM could be summarized in the following: the main degradation step begins at 250°C, followed by a short plateau at 400°C for the former, and main degradation step for the latter between 400 and 500°C. As stated previously, this behavior is partly attributed to the presence of OP and therefore to a higher surface area exposed to degradation. From 500 to 550°C the foam NaCl 60-80 evidences a relative decrease of rubber mass loss, similarly to the other foams with an almost sequential thermolysis of carbon black up to 650°C. The higher final residue at 700°C of NaCl 60-80 foam (around 6 wt%) is directly dependent on the residual salt in the rubber matrix. As given in Table 3, the amount of residual salt should be around 7 wt% and this difference may be due to the inhomogeneous distribution of salt residues within the sample.

3.2.6 | Thermal conductivity measurements

Thermal conductivity of EPDM unfoamed sample and of the prepared foams was measured both through guarded hot plate and hot disk technique, and the most important results are shown in Figure 10.

For unfoamed EPDM significantly higher values were obtained (0.503 W/mK by using Guarded Hot Plate and 0.285 W/mK by using the Hot Disk). The different values obtained with the two techniques can be attributed to their lower accuracy at high thermal conductivity values.

TABLE 6 Selected results of the TGA tests

Sample	$T_{2\%}$ (°C)	T_{peak1} (°C)	T_{peak2} (°C)	m_{250} (wt%)	m_{415} (wt%)	m_{500} (wt%)	m_{700} (wt%)
EPDM	231.3	—	460.5	97.5	89.7	22.0	3.6
NaCl 60–80	230.0	363.6	452.2	97.2	51.0	31.7	5.9
Micropearl	219.1	350.0	453.0	97.0	75.4	27.9	3.7
Expancel	222.6	327.7	469.4	97.3	77.3	29.0	3.3

Abbreviations: EPDM, ethylene propylene diene monomer; TGA, thermogravimetric analysis.

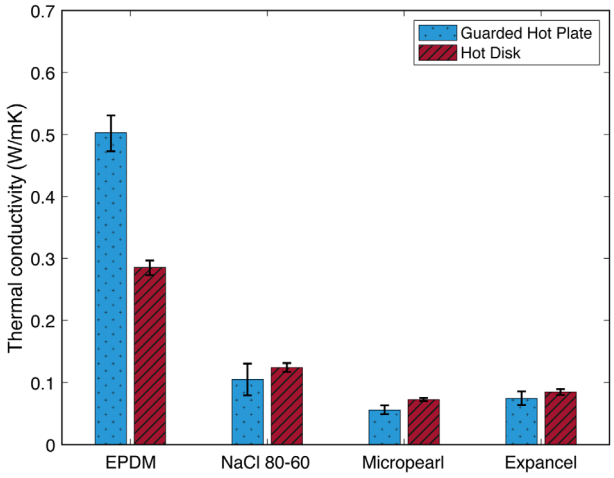

FIGURE 10 Results of the thermal conductivities tests [Color figure can be viewed at wileyonlinelibrary.com]

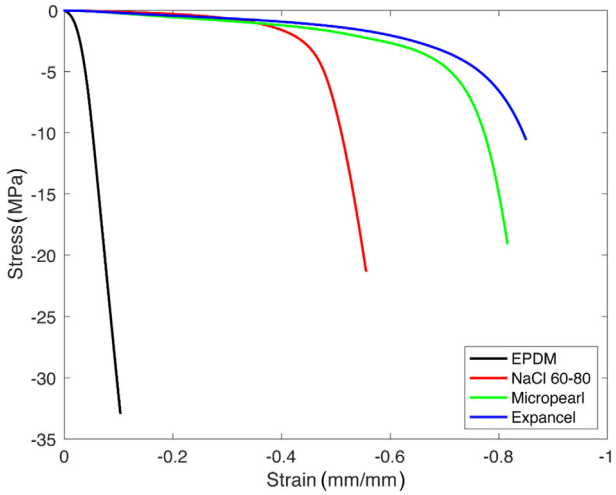

FIGURE 11 Representative stress-strain curves from quasi-static compression tests. EPDM, ethylene propylene diene monomer [Color figure can be viewed at wileyonlinelibrary.com]

Thermal conductivities of the sample NaCl 60-80 obtained through the two different testing techniques (0.11 and 0.13 W/mK) are comparable, and are quite similar to those of Micropearl (0.07 and 0.09 W/mK) and Expancel (0.09 and 0.10 W/mK). Despite the presence of OP, the sample NaCl 60-80 is characterized by appreciable low conductivity values and it can be considered as a valuable material for thermal insulation applications.

3.2.7 | Quasi-static compression test and shore hardness measurements

Compressive behavior of unfoamed EPDM vs foamed samples are remarkably different as shown in Figure 11 and Table 7. Values of ε_5 show that unfoamed EPDM undergoes a rapid increase of the stress even at low deformation values, unlike the expanded samples whose curves show a very large stress plateau at limited strain levels. The large stress plateau is due to the progressive deformation of the porosity as densification occurs, causing a great increase in stress with strain at certain strain values; the samples the strain at which densification starts for Micropearl and Expancel (∼0.7 and ∼ 0.8 mm/mm, respectively) is higher than for the sample produced through salt leaching (∼0.4 mm/mm), because of the formers' lower density values. As expected, the elastic moduli of the foamed samples are lower than the modulus of the unfoamed EPDM sample. Values of $\sigma_{0.15}$ and $\sigma_{0.35}$ is the highest for Micropearl between the foamed samples while lowest for NaCl 60-80. This modulus behavior is caused by residual microcapsule parts resulting in an increase of the elastic modulus and stress for the Micropearl and Expancel samples respect to the NaCl 60-80. Shore A values, also reported in Table 7, show the same trend. In particular NaCl 60-80 shows the lowest value, followed by Expancel, Micropearl and unfoamed EPDM. Low hardness of NaCl 60-80 reflects the high porosity content of this material. Moreover, OP causes lower Shore A hardnesses.

3.2.8 | Compression set measurements

Permanent deformation values obtained from compression set tests (CS) given in Table 8 show that all foamed samples show lower recovery properties than bulk EPDM rubber (8%). Expancel and Micropearl samples present

TABLE 7 Shore A hardness and normalized results of the quasi-static compression tests

Sample	Shore A (–)	E (MPa cm^3/g)	$\sigma_{0.15}$ (MPa cm^3/g)	$\sigma_{0.35}$ (MPa cm^3/g)	ε_5 (mm/mm)
EPDM	60.7 ± 0.3	404 ± 43	/	/	−0.05 ± 0.01
NaCl 60–80	9.9 ± 1.7	4.2 ± 0.9	0.42 ± 0.09	2.26 ± 0.57	−0.49 ± 0.03
Micropearl	35.9 ± 2.7	18.0 ± 4.8	2.32 ± 0.92	5.14 ± 1.29	−0.69 ± 0.03
Expancel	29.4 ± 2.0	10.9 ± 3.1	1.24 ± 0.33	3.04 ± 0.37	−0.79 ± 0.02

Abbreviation: EPDM, ethylene propylene diene monomer.

TABLE 8 Results of the compression set on the prepared samples

Sample	Compression set (%)
EPDM	8.3 ± 0.3
NaCl 60-80	12.0 ± 1.3
Micropearl	31.2 ± 1.1
Expancel	59.1 ± 1.9

Abbreviation: EPDM, ethylene propylene diene monomer.

very high CS values (31% and 59%, respectively). These higher permanent deformation values have been attributed to the collapse of the close cells under compression. On the contrary, the open foam structure obtained by salt leaching method is certainly the main reason for the low compression set value of NaCl 60-80, similar to that obtained for the unfoamed EPDM. Low compression set values suggest applications in cyclic compression conditions.

3.2.9 | Modeling of the compressive properties

Modeling of the compressive behavior of the produced materials has been carried out in order to better investigate the influence of the foaming process on the prepared foams. The Mooney-Rivlin depending on the number of parameters, can model curves having different shapes. Mooney-Rivlin equation with 2 parameters (MR 2), with 3 parameters (MR 3), and with 5 parameters (MR 5) were used. Applying the hypothesis of incompressible and isotropic materials and the condition of uniaxial load the following Mooney-Rivlin equations with 2, 3, 5 terms can be obtained;[46-48] they are expressed in terms of stress (σ) as function of stretch (λ), as shown in Equations (10), (11), and (12) where $C_{\#\#}$ represents a fitted parameter.

$$\sigma = 2C_{10}\left(\frac{\lambda^3-1}{\lambda^2}\right) + 2C_{01}\left(\frac{\lambda^3-1}{\lambda^3}\right) \tag{10}$$

$$\sigma = 2C_{10}\left(\frac{\lambda^3-1}{\lambda^2}\right) + 2C_{01}\left(\frac{\lambda^3-1}{\lambda^3}\right) + 6C_{11}\left(\lambda^2-\lambda-1-\frac{1}{\lambda^4}+\frac{1}{\lambda^3}+\frac{1}{\lambda^2}\right) \tag{11}$$

$$\sigma = 2C_{10}\left(\frac{\lambda^3-1}{\lambda^2}\right) + 2C_{01}\left(\frac{\lambda^3-1}{\lambda^3}\right) + 6C_{11}\left(\lambda^2-\lambda-1-\frac{1}{\lambda^4}+\frac{1}{\lambda^3}+\frac{1}{\lambda^2}\right) + 4C_{20}*\lambda*\left(1-\frac{1}{\lambda^3}\right)\left(\lambda^2+\frac{2}{\lambda}-3\right) + 4C_{02}\left(2\lambda+\frac{1}{\lambda^2}-3\right)\left(1-\frac{1}{\lambda^3}\right) \tag{12}$$

A second model was used as alternative to the more common Mooney-Rivlin model: the exponential-logarithmic model.[49,50] A simple mathematical formulation based on exponential and logarithmic functions is used and has the advantage of relating model parameters to physical quantities and has three fitted parameters, A, a and b. Applying the hypothesis of incompressible and isotropic materials and the condition of uniaxial load[49] the model can be expressed as shown in Equation (13):

$$\sigma = \left(\frac{\lambda^3-\lambda}{\lambda}\right)*2A*\left[e^{a\left(\frac{\lambda^3+2-3\lambda}{\lambda}\right)} - b\ln\frac{\lambda^3+2-2\lambda}{\lambda}\right] \tag{13}$$

The experimental data from compression tests on unfoamed EPDM sample and the fitting of these curves through theoretical models (see Equations (10)-(13)) are compared in Figure 12(A). The Mooney-Rivlin model gives a good fit to experimental data, and fitting quality improves with increasing the number of parameters. The interpolation is already acceptable with two terms although it diverges at large stretch values; increasing the number of material parameters the accuracy of the model increases also at high stretch values. Looking at the curves obtained for NaCl 60-80, Micropearl and Expancel samples respectively reported in Figure 12(B-D) shows

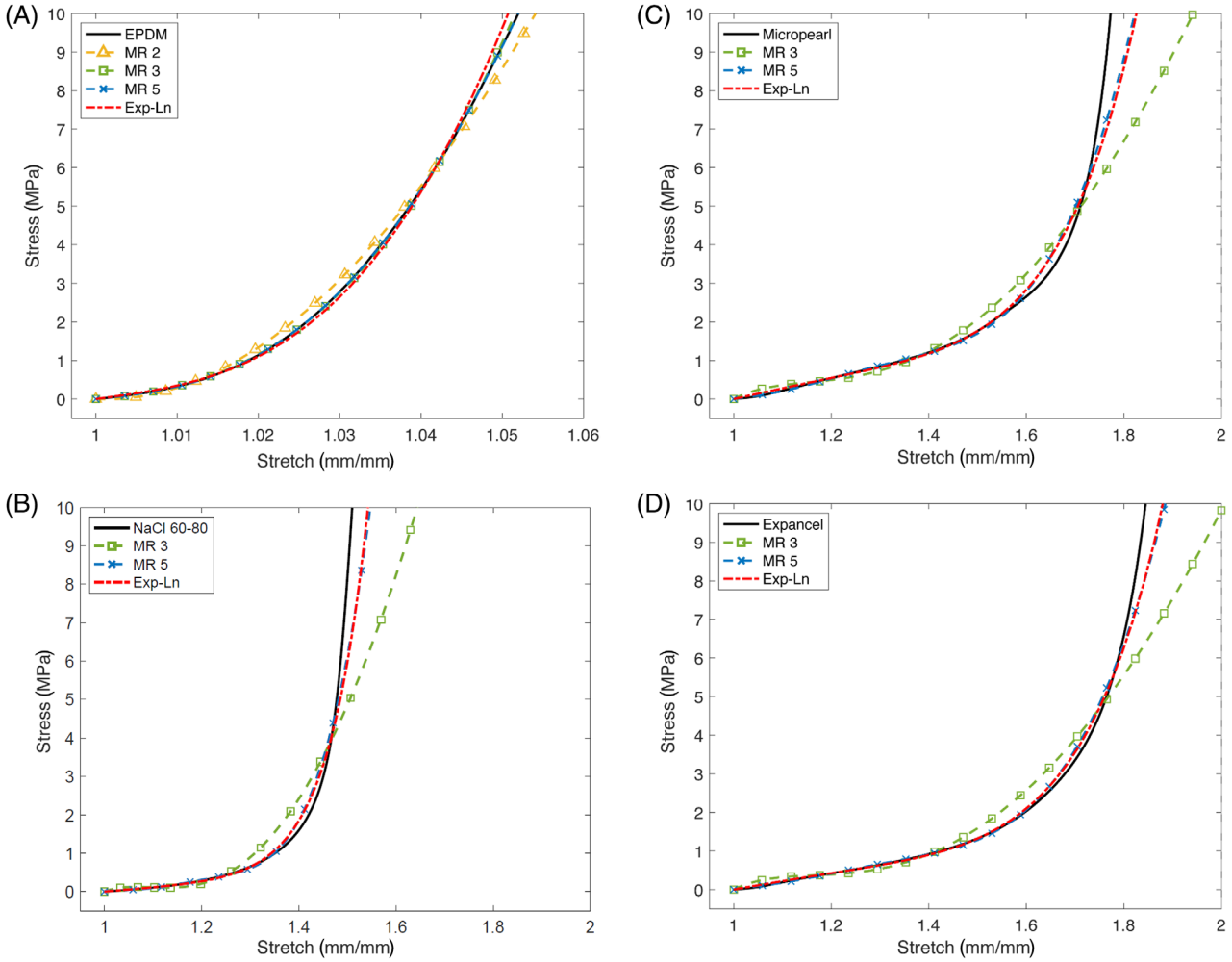

FIGURE 12 Theoretical predictions of the compressive curves according to the Mooney-Rivlin and Exp-Ln models: ethylene propylene diene monomer (EPDM) (A), NaCl 60-80, (B), Micropearl (C), Expancel (D) [Color figure can be viewed at wileyonlinelibrary.com]

that the Mooney-Rivlin model requires at least three terms to obtain acceptable agreement with experimental data ($R^2 = 0.9996$) even though the MR 3 equation still fails to predict the material behavior at large stretch levels. Good interpolations at high stretch values can be obtained by using MR 5 ($R^2 = 0.99998$) and Exp-Ln models ($R^2 = 0.99998$). Calculations with the Exp-Ln model are easier and quicker because of a lower number of fitting parameters. In Table 9 the fitting parameters and the coefficient of determination R^2 for each model applied to compressive stress-strain curves of the prepared samples.

Kumar et al. attributed the increase of C_{10} to the rubber hardening due to crosslinking.[46] C_{10} is lower for the foamed samples, meaning that samples that are porous are characterized by an apparent lower cross-linking values, which is in fact misleading since porosity will lead to a lower C_{10}. C_{01} represents the deviation from elastic behavior: as it increases, nonlinearity in stress-strain curve increases.[46] This parameter is highest for NaCl 60-80 as given in Table 9. As shown in Figure 10, the stress-strain curve for this material is characterized by a very rapid change in slope of the stress-strain curve at high strain values.

The parameters of the Exp-Ln model are a, A and b: A refers to the small deformation region and it is related to the crosslinking degree; the parameter b affects the middle section of the stress-strain curve and by increasing this parameter the curve progressively approaches the behavior of rubber foams, while at large deformation the compressive behavior is mainly determined by the parameter a, related to the chain extensibility.[49] The parameter A is maximum in the case of unfoamed EPDM and lower for the foamed samples: as previously observed this small value is not related to a lower crosslinking degree but rather higher porosity. The parameter b is minimum in the case of unfoamed EPDM and higher for the expanded samples (especially in the

TABLE 9 Fitting parameters obtained from the modeling of compressive curves of the prepared samples

Samples	Constitutive model	Material parameters	R^2
EPDM	MR 2	$C_{10} = 662.2$	0.99999
		$C_{01} = 663.8$	
	MR 3	$C_{10} = 166.2$	0.99999
		$C_{01} = -163.2$	
		$C_{11} = 1546.7$	
	MR 5	$C_{10} = 38.4$	0.99999
		$C_{01} = -34.7$	
		$C_{11} = 86\ 658.5$	
		$C_{20} = -48\ 677.6$	
		$C_{02} = -35\ 468.3$	
	Exp-Ln	$A = 4.7$	0.99999
		$a = -0.0049$	
		$b = -796.3$	
NaCl 60–80	MR 3	$C_{10} = -9.1$	0.99963
		$C_{01} = 9.9$	
		$C_{11} = 5.8$	
	MR 5	$C_{10} = -10.2$	0.99998
		$C_{01} = 10.6$	
		$C_{11} = -424.0$	
		$C_{20} = 166.5$	
		$C_{02} = 278.7$	
	Exp-Ln	$A = 0.18$	0.99998
		$a = 4.3$	
		$b = 3.4$	
Micropearl	MR 3	$C_{10} = -5.3$	0.99960
		$C_{01} = 6.4$	
		$C_{11} = 2.4$	
	MR 5	$C_{10} = -1.6$	0.99997
		$C_{01} = 2.0$	
		$C_{11} = -76.6$	
		$C_{20} = 27.9$	
		$C_{02} = 54.7$	
	Exp-Ln	$A = 0.47$	0.99996
		$a = 1.2$	
		$b = 1.7$	
Expancel	MR 3	$C_{10} = -5.3$	0.99959
		$C_{01} = 6.4$	
		$C_{11} = 2.2$	
	MR 5	$C_{10} = -2.2$	0.99998
		$C_{01} = 2.6$	
		$C_{11} = -55.9$	
		$C_{20} = 20.2$	
		$C_{02} = 40.8$	
	Exp-Ln	$A = 0.37$	0.99998
		$a = 1.1$	
		$b = 1.8$	

Abbreviation: EPDM, ethylene propylene diene monomer.

case of NaCl 60-80 foam). These results confirm the foamed nature of the three materials, with the NaCl 60-80 that seems more similar to a rubber foam (due to the high value of the parameter *b*). The parameter *a* shows the lowest values for unfoamed EPDM and the highest for NaCl 60-80: these values can be related to the higher chain extensibility of foamed samples (especially in the case of NaCl 60-80).

4 | CONCLUSIONS

A reliable method to obtain foamed EPDM rubber samples through salt leaching was demonstrated. The technique turned out to be easy and repeatable and a possible substitute for the traditional foaming agents. SEM micrographs and density measurements, followed by porosity and connectivity evaluation, showed that the morphology of the foams produced with this technique were constituted by an open, highly interconnected porosity. Water uptake tests highlighted that smaller pores are responsible for the absorption of a higher quantity of water with respect to the pores having higher dimensions. Thermal conductivities of foamed rubber produced by salt leaching are low and similar to those of the samples obtained using commercial foaming agents. Compression tests showed that expanded samples presented a very large stress plateau starting at low strain values. In particular, the sample obtained via salt leaching presented the lowest elastic modulus and a stress increase occurring at lower deformation values with respect to samples obtained by using conventional foaming agents. The open foam structure obtained by salt leaching method led to low residual deformation values similar to those of the unfoamed EPDM sample confirming the good crosslinking degree. The modeling of the compression curves using the Mooney-Rivlin model (MR) and an Exponential-Logarithmic (Exp-Ln) model showed fits. In comparison with traditionally expanded materials, these novel foams possess good thermomechanical properties and can be thus applied for thermal insulation purposes.

ACKNOWLEDGEMENTS

Erika Bordignon is gratefully acknowledged for the drawings and the graphical cooperation, Ms. Claudia Gavazza for the acquisition of SEM micrographs and Prof. Maurizio Grigiante for the use of the Hot Disk thermal analyser.

ORCID

Francesco Valentini https://orcid.org/0000-0001-9496-0501

REFERENCES

[1] B. Q. Wang, Z. L. Peng, Y. Zhang, Y. X. Zhang, *Plast. Rubber Compos.* **2006**, *35*(9), 360.
[2] L. Kenens; C. Warmeling. VDI-Gesellschaft Kunststofftechnik, Braunschweig, **1997**.
[3] W. Michaeli, S. Sitz, *Cell. Polym.* **2010**, *29*(4), 227.
[4] D. Klempner, K. C. Frish, *Handbook of Polymeric Foams and Foam Technology*, Carl Hanser Verlag, München, Germany **1991**.
[5] L. Wahlen Blowing Agents and Foaming Processes Munich, **2006**.
[6] F. Röthemeyer, F. Sommer, *Kautschuk Technologie, Werkstoffe - Verarbeitung-Produkte*, Carl Hanser Verlag, München, Germany **2013**.
[7] H. Saechtling, *Manuale Delle Materie Plastiche*, Tecniche Nuove, Milano, Italy **2006**.
[8] J. Stehr, *Gummi Fasern Kunststoffe* **2015**, *68*(12), 821.
[9] C. Hopmann, F. Lemke, Q. Nguyen Binh, *J. Appl. Polym. Sci.* **2016**, *133*(27), 1.
[10] J. A. Reglero Ruiz, M. Vincent, J.-F. Agassant, T. Sadik, C. Pillon, C. Carrot, *Polym. Eng. Sci.* **2015**, *55*(9), 2018.
[11] N. Mills, *Polymer Foams Handbook: Engineering and Biomechanics Applications and Design Guide*, Butterworth-Heinemann, Oxford, UK **2007**.
[12] A. Vahidifar, S. N. Khorasani, C. B. Park, H. E. Naguib, H. A. Khonakdar, *Ind. Eng. Chem. Res.* **2016**, *55*(8), 2407.
[13] E. Wimolmala, K. Khongnual, N. Sombatsompop, *J. Appl. Polym. Sci.* **2009**, *114*(5), 2816.
[14] W. Yamsaengsung, N. Sombatsompop, *J. Macromol. Sci. Phys.* **2008**, *47*(5), 967.
[15] A. Dutta, M. Cakmak, *Rubber Chem. Technol.* **1992**, *65*(5), 932.
[16] M. A. Bashir, M. Shahid, R. A. Alvi, A. G. Yahya, *Key Eng. Mater.* **2012**, *510-511*, 532.
[17] N. N. Najib, Z. M. Ariff, A. A. Bakar, C. S. Sipaut, *Mater. Des.* **2011**, *32*(2), 505.
[18] K.-C. Choi, J.-H. Kim, J.-M. Yoon, S.-Y. Kim, *Elastomers Compos.* **2006**, *41*(3), 198.
[19] S.-S. Choi, B.-H. Park, H. Song, *Polym. Adv. Technol.* **2004**, *15*, 122.
[20] C. Nah, W. D. Kim, W. Lee, *Korea Polym. J.* **2001**, *9*, 157.
[21] A. M. Y. E. Lawindy, K. M. A. El-Kade, W. E. Mahmoud, H. H. Hassan, *Polym. Int.* **2002**, *51*(7), 601.
[22] W. E. Mahmoud, M. H. I. El-Eraki, A. M. Y. El-Lawindy, H. H. Hassan, *J. Phys. D Appl. Phys.* **2006**, *39*(3), 541.
[23] B. S. Zhang, X. F. Lv, Z. X. Zhang, Y. Liu, J. K. Kim, Z. X. Xin, *Mater. Des.* **2010**, *31*(6), 3106.
[24] E. Bardy, J. Mollendorf, D. Pendergast, *J. Phys. D Appl. Phys.* **2005**, *38*, 3832.
[25] W. Yamsaengsung, N. Sombatsompop, *Compos. Part B Eng.* **2009**, *40*(7), 594.
[26] Z. Zakaria, Z. M. Ariff, T. L. Hwa, C. S. Sipaut, *Malaysian Polym. J.* **2007**, *2*(2), 22.
[27] M. S. Sohn, K. S. Kim, S. H. Hong, J. K. Kim, *J. Appl. Polym. Sci.* **2003**, *87*, 1595.
[28] C. Komalan, K. E. George, P. A. S. Kumar, K. T. Varughese, S. Thomas, *Express Polym. Lett.* **2007**, *1*(10), 641.
[29] S. Datta, *Synthetic Elastomers*, Rapra Technology Ltd, Shawbury, UK **2001**.
[30] F. Deng, H. Jin, L. Zhang, Y. He, *J. Elastomers Plast.* **2020**, *20*(10), 1.

[31] D. Kropp, W. Michaeli, T. Herrmann, O. Schröder, *J. Cell. Plast.* **1998**, *34*, 304.
[32] R. Gendron, M. F. Champagne, Y. Delaviz, M. E. Polasky, *J. Cell. Plast.* **2006**, *42*, 127.
[33] S. H. Oh, S. G. Kang, E. S. Kim, S. H. Cho, J. H. Lee, *Biomaterials* **2003**, *24*, 4011.
[34] R. Scaffaro, F. Lopresti, L. Botta, S. Rigogliuso, G. Ghersi, *Macromol. Mater. Eng.* **2016**, *301*(2), 182.
[35] R. Scaffaro, F. Lopresti, L. Botta, S. Rigogliuso, G. Ghersi, *J. Mech. Behav. Biomed. Mater.* **2016**, *54*, 8.
[36] S. G. Mosanenzadeh, H. E. Naguib, C. B. Park, N. Atalla, *Polym. Eng. Sci.* **2013**, *53*(9), 1979.
[37] R. Scaffaro, F. Lopresti, L. Botta, S. Rigogliuso, G. Ghersi, *J. Mech. Behav. Biomed. Mater.* **2016**, *63*, 303.
[38] R. Kroon, J. D. Ryan, D. Kiefer, L. Yu, J. Hynynen, E. Olsson, C. Müller, *Adv. Funct. Mater.* **2017**, *27*(47), 1704183.
[39] W. Trakanpruk, Y. Rodthong, *J. Met. Mater.* **2008**, *18*(2), 33.
[40] Q. Chen, J. Zhao, J. Ren, L. Rong, P. F. Cao, R. C. Advincula, *Adv. Funct. Mater.* **2019**, *29*(23), 1900469.
[41] F. Valentini, A. Dorigato, A. Pegoretti, *Rubber Chem. Technol.* accepted for publication.
[42] E1225-13 standard test method for thermal conductivity of solids using the guarded- comparative-longitudinal heat flow technique, **2013**.
[43] J. R. White, S. K. De, *Rubber Technologist's Handbook*, Rapra Technology Ltd, Shawbury, UK **2001**.
[44] R. Scaffaro, F. Lopresti, L. Botta, A. Maio, *Composites, Part B* **2016**, *98*, 70.
[45] F. X. Alvarez, D. Jou, A. Sellitto, *Appl. Phys. Lett.* **2010**, *97*(3), 33103.
[46] N. Kumar, R. V. Venkateswara, *Int. J. Mech. Eng.* **2016**, *6*(1), 43.
[47] G. Marckmann, E. Verron, *Rubber Chem. Technol.* **2006**, *79* (5), 835.
[48] L. Andena, F. Briatico-Vangosa, E. Cazzoni, A. Ciancio, S. Mariani, A. Pavan, *Sports Eng.* **2015**, *18*(1), 1.
[49] H. Khajehsaeid, J. Arghavani, R. Naghdabadi, *Eur. J. Mech. A Solids* **2013**, *38*, 144.
[50] L. J. Hart-Smith, *Z. Angew. Math. Phys.* **1966**, *17*, 608.

How to cite this article: Zonta E, Valentini F, Dorigato A, Fambri L, Pegoretti A. Evaluation of the salt leaching method for the production of ethylene propylene diene monomer rubber foams. *Polym Eng Sci*. 2021;61:136–153. https://doi.org/10.1002/pen.25563